TOXICOLOGICAL SCIENCES **138(2)**, 333–343 2014
doi: 10.1093/toxsci/kft336
Advance Access publication January 2, 2014

A Real-time Impedance-Based Screening Assay for Drug-Induced Vascular Leakage

Stefan Kustermann,[*,1] Tobias Manigold,[*,†] Corinne Ploix,[*] Marion Skubatz,[*] Tobias Heckel,[*] Heather Hinton,[*] Thomas Weiser,[*] Thomas Singer,[*] Laura Suter,[*,‡] and Adrian Roth[*]

**F. Hoffmann-La Roche Ltd, 4070 Basel, Switzerland; †Department of Internal Medicine, University Hospital Basel, 4031 Basel, Switzerland; and ‡Institute for Chemistry and Bioanalytics, School of Life Sciences, 4132 Muttenz, Switzerland*

[1]To whom correspondence should be addressed at F. Hoffmann-La Roche Ltd, Grenzacherstrasse 124, 4070 Basel, Switzerland. Fax: +41 61 688 8101. E-mail: stefan.kustermann@roche.com.

Received October 31, 2013; accepted December 20, 2013

Vascular leakage is a serious side effect of therapies based on monoclonal antibodies or cytokines which may lead to life-threatening situations. With the steady increase of new drug development programs for large molecules, there is an urgent need for reliable tools to assess this potential liability of new medicines in a rapid and cost-effective manner. Using human umbilical vein endothelial cells (HUVECs) as a model for endothelium, we established an impedance-based assay measuring the integrity of the endothelial cell monolayer in real time. We could demonstrate that the HUVEC monolayer in our system was a relevant model as cells expressed major junctional proteins known to be responsible for maintaining tightness as well as receptors targeted by molecules known to induce vascular leakage *in vivo*. We assessed the time-dependent loss of barrier function using impedance and confirmed that signals obtained corresponded well to those from standard transwell assays. We assayed a series of reference molecules which led to the expected change of barrier integrity. A nonspecific cytotoxic effect could be excluded by using human fibroblasts as a non-responder cell line. Finally, we could show reversibility of vascular permeability induced by histamine, IL-1β, or TNF-α by coincubation with established antagonists, further demonstrating relevance of this new model. Taken together, our results suggest that impedance in combination with HUVECs as a specific model can be applied to assess clinically relevant vascular leakage on an *in vitro* level.

Key Words: **HUVEC; barrier function; drug development; mab.**

The inner layer of the vascular wall is constituted of endothelial cells that represent the physical barrier between blood and interstitial tissue. Endothelial cells are closely connected with their neighboring cells by so-called tight and adherens junctions which are responsible for maintaining the tightness of the vasculature (Vandenbroucke *et al.*, 2008). Thus, modulation of these junctions has a direct impact on the permeability of the vasculature. For example, during inflammatory processes in the body a release of proinflammatory cytokines can lead to an impairment of the vascular barrier function (Aghajanian *et al.*, 2008; Dudek and Garcia, 2001) and lead to vascular leak syndrome (VLS) either by direct or by cell-mediated mechanisms. Other vasoactive substances, such as histamine and thrombin, can also affect the stringency of the endothelial barrier and can also trigger signaling cascades that downregulate tight and adherens junction proteins and cytoskeletal remodeling (Aghajanian *et al.*, 2008). These processes weaken endothelial cell connections and lead to a separation of cells and looseness of the barrier for a limited time. Reduced integrity of the vascular endothelial monolayer then finally causes a leakage of fluid from the circulatory system into the interstitial space which results in interstitial edema, decrease in microcirculatory perfusion, deprivation of intravasal volume and eventually to organ dysfunction, and in an extreme case systemic shock (Bazzoni, 2006; Capaldo and Nusrat, 2009).

Although observed under selected pathological conditions, vascular leakage can also occur during infusion reactions after administration of monoclonal antibodies or cytokines. Although reversible when managed early enough, this may lead to a life-threatening response as seen in patients who suffered from cytokine storm after receiving the superagonistic anti-CD28 antibody TGN1412 during a phase I trial (Suntharalingam *et al.*, 2006). It has been shown that VLS is one of the dose-limiting side effects of IL-2 in cancer patients or HIV patients receiving highly active antiretroviral therapy (Baluna, 2007; Kovacs *et al.*, 1995; Lotze *et al.*, 1986; Siegel and Puri, 1991). Because preclinical safety characterization of therapeutic cytokines and monoclonal antibodies becomes increasingly more important during development, there is a need for systems with the potential to assess vascular leakage early on. Today's standard assay to measure vascular permeability induced by drugs is by comparing diffusion rates of a dye through a monolayer of an endothelial cell of treated and untreated cells (Ludwig *et al.*, 2011). Although technically correct, this assay is cumbersome and its throughput is low.

The goal of the present study was to design an *in vitro* system based on human umbilical vein endothelial cells (HUVECs) as

a model to assess the potential of drug candidates to induce vascular leakage. By using an impedance-based approach, we were aiming at measuring drug-induced effects affecting the tightness of endothelial cell-cell junctions although passage of fluid or macromolecules were only indirectly reflected by the readout. We herein demonstrate that our impedance-based platform captures monolayer changes associated with disruption of tight and adherens junctions which are in full agreement to those captured by passive diffusion of FITC (Fluorescein isothiocyanate) -coated beads in a transwell chamber. In addition, this noninvasive method allows real-time kinetics, dose-effect comparison, parallel recording of different treatments, and semiquantitative assessment relative to controls in a very easy and efficient way. Specifically, we analyzed eight different cytokines and vasoactive substances, and our impedance-based results concord with literature reports. Importantly, we also demonstrate that the impedance-based assay was able to monitor the reversibility of the vascular leakage induced by IL-1β, TNF-α, or histamine when applying selective antagonists such as anakinra, remicade, clemastine, and methylprednisolone. Taken together, in the present study we could establish an easy and robust system that is able to assess vascular leakage in a real-time fashion. This system could be of importance for the pharmaceutical industry not only to screen drugs early on for their potential to induce vascular leakage in humans but also to select for the best antidote treatment or to perform mechanistic investigations.

MATERIALS AND METHODS

Material. HUVECs and specific culture medium (EGM2) were purchased from Lonza. Thrombin and histamine were purchased from Sigma-Aldrich and human recombinant cytokines were purchased from rnd systems, with the exception of IFN-γ from Roche. Antagonists as methylprednisolone (brand name: Solu-Medrol) were purchased from Pfizer, clemastine (brand name: Tavegil) from Novartis, anakinra (brand name: Kineret) from Sobi, Infliximab (brand name: Remicade) from Janssen Biotech, E-Plates View from Roche Applied Science and Collagen I, and rat tail from BD.

Cell culture. HUVECs were cultured at 37°C, 5% CO_2, and 95% humidity in EGM2 medium (Lonza) until they reached a confluency of maximal 80% and subsequently subcultivated. All experiments were performed with cells between passages 2 and 8. Human fibroblast cell line CCD25-SK (ATCC CRL-1474) was grown in MEM (Minimum Essential Media) (Gibco) containing 10% FCS (Fetal Calf Serum) and 2mM L-Glutamine. Medium was exchanged every other day and cells were subcultured before they reached complete confluence.

Transwell assay for vascular permeability. To analyze a thrombin-induced increase in endothelial permeability, HUVECs were grown on collagen-coated transwell inserts with a pore size of 0.4 μm (Millipore). For collagen coating, filters were incubated with 200 μl 50 μg/ml rat tail collagen (BD) for 1 h at room temperature. Before cells were seeded, inserts were washed once with phosphate buffered saline (PBS). Cultures were grown to complete confluence, controlled by visual inspection which was normally after one week. During this period medium was changed every other day. To measure transwell permeability, 150 kDa FITC-labeled Dextran (Fluorescein isothiocyanate–dextran, Sigma) was added to a final concentration of 7.5 μg/well to the upper part of the transwell system. At 60 and 30 min before thrombin was added, samples were taken for measuring baseline transwell permeability, each 10 μl in triplicates from the lower chamber. Samples were transferred to a black wall 384 multiwell plate for final fluorescence analysis. Afterward thrombin was added to the upper part of the transwell insert to a final concentration of 20 U/ml. Following thrombin treatment, three samples were taken at 0, 30, 45, 60, 75, 120, 150, and 210 min for each well and were again transferred to a 384 well plate for later fluorescence measurement. Fluorescence was measured using an Envision Plate reader (Perkin Elmer) at 488 nm excitation and 555 nm Emission. Slope was determined from mean fluorescence values of three technical replicates between two adjacent time points for each experiment separately. Each experiment was done in triplicate and data are displayed as slope ± standard deviation for untreated and thrombin-treated HUVECs separately.

High content image analysis for cell death. To determine the amount of dead cells at the end of the impedance experiment, a LIVE/DEAD fixable cell stain (Life Technologies) was used in combination with high content imaging on an Array Scan VTi Platform (Thermo Fisher). LIVE/DEAD assay was used as recommended by the vendor (Invitrogen). Briefly HUVECs, 24 h after the final addition of the antagonist, were washed with PBS (Life Technologies) and then incubated with the reconstituted dye diluted 1:1000 in Hank's balanced salt solution (Life Technologies) for 30 min at room temperature and in the dark. Afterward cells were washed, fixed for 15 min with 4% PFA (Paraformaldehyde 16% Alfa Aesar, 1:4 in PBS), and cell nuclei were counterstained with Hoechst 33342 (diluted 1:2000 in PBS; Life Technologies). Afterward the E-Plate View was imaged using a x20 magnification and analyzed using the Target Activation Bioapplication with Hoechst in channel 1 as objects with BGRFR_386 filters. In channel 2, nuclear fluorescence intensity of LIVE/DEAD cell stain was assessed with BGRFR_485 filters. Percent positive responders for dead cells were calculated from cells identified as objects in channel 1 (nuclei) and showing a mean total intensity above 50,000 in channel 2 (dead cell stain). Results were calculated as the average of four analyzed wells, in each well 28 fields were analyzed and displayed as the percentage of dead cells ± standard deviation.

xCELLigence assay for vascular permeability. For impedance analysis, HUVECs or CCD25-SK were seeded

on E-Plates View (Roche Applied Science) at a density of 2,000 cells/well or 2500 cells/well, respectively. During the following seven days, cells were grown to confluence indicated by a plateau of the impedance curve. During that time medium was changed every other day and impedance termed "cell index" (CI) was measured every 15 min. HUVECs or CCD25-SK were treated with cytokines or other compounds at three different concentrations as indicated in the graphs and the Results section. After treatment, impedance was measured every 2 min for the following 12 h. All HUVEC experiments were done with two different batches of HUVECs. For analysis, impedance values were calculated as baseline normalized impedance as follows: for each time point average impedance value of untreated controls was subtracted and normalized as $CI_{(normalized)} = CI_{time\ x} / CI_{norm\ time}$ (termed here "baseline normalized CI"). This baseline normalized CI was used for graphical result representation using Microsoft Excel 2010. Results were displayed as the average of four or six independent wells treated with the indicated compounds and for Figures 1C and 1D ± standard deviation.

For rescue/inhibition experiments, HUVECs were cultivated as mentioned above. At time point 1 (see Fig. 4), eight wells were treated with "inhibitors" anakinra (final concentration 1 μg/ml), Remicade (final concentration 200 μg/ml), Tavegil (final concentration 700 ng/ml), or Methyl-Prednisolone (final concentration 40 μg/ml). At time point 2, a subset of 4 wells of the previously 8 treated wells, IL-1β, histamine, or TNF-α was added and eight additional wells were treated with IL-1, TNF, and histamine alone. Impedance analysis was continued for the following 12 h. Then, impedance measurements were paused and four of the eight wells, treated with histamine, IL-1β, or TNF-α before, were now treated with the corresponding antagonists in the same concentration as mentioned above. E-Plates were put back into the incubator and impedance measurements were continued for the following 12 h. At the end of the experiments, E-Plates were further processed for a LIVE/DEAD assay as mentioned above. Finally impedance values were calculated as mentioned above except for baseline CI calculation. For calculation of baseline CI, impedance values of the corresponding antagonist alone were used as control values. Data were transferred to Microsoft Excel and graphs represent average values of four replicates.

Immunocytochemistry and microscopy. For immunocytochemistry experiments, cells were seeded on collagen-coated eight-well chamber slides (10 μg/cm^2 rat tail collagen for 1 h at room temperature; BD Falcon) at a density of 2000 cells/chamber. Cells were grown until they reached complete confluence that was after eight days and medium was exchanged every other day. Cells were treated with thrombin (20 U/ml) for 30 min whereas controls were left untreated. For immunocytochemistry, cells were washed once with PBS and afterward fixed with 2% PFA for 5 min at room temperature and then washed once with PBS and permeabilized for 5 min with 0.1% PBST (PBS, Triton-X 100 added 0.1% v/v) and blocked for 30 min with 10% normal goat serum in PBS. First antibody was diluted in PBS (Claudin 5 1:100, ZO-1 1:100, and VE-Cadherin 1:50) incubated overnight at 4°C and after three washing steps with PBS secondary antibody Alexa 488 or 555 anti-mouse (1:200 in PBS) was added for 1 h at room temperature. After three final washing steps with PBS slides were coversliped with Prolong Gold Antifade (Invitrogen) containing DAPI (4′,6-Diamidin-2-phenylindol) as a nuclear stain. For actin staining slides were incubated with Alexa 647 labeled Phalloidin as recommended by the manufacturer (Invitrogen). Images were taken with a confocal microscope (DMI 4000B, Leica) at x40 magnification and are displayed as projections of multiple Z-layers. Specificity of antibody staining was proven by omitting primary antibodies for control samples and incubation with secondary antibody only. This procedure did not reveal any unspecific staining for all secondary antibodies used in the present study.

Gene expression analysis in HUVECs. Total RNA from cells was extracted using the RNeasy Mini kit combined with DNase treatment on a solid support (Qiagen). RNA quality assessment and quantification was performed using microfluidic chip analysis on an Agilent 2100 bioanalyzer (Agilent Technologies). Five micrograms of total RNA was reverse transcribed using the Roche cDNA Synthesis System. After silica adsorption column purification, double-stranded cDNA was labeled with Cy3 using the Roche NimbleGen One Color DNA Labeling Kit. NimbleGen 12 × 135K gene expression microarrays (100718_HG18_opt_expr) were hybridized with 4 μg of Cy3-labeled cDNA for 16 h at 42°C and were washed and dried according to the manufacturer's instruction. Microarray data were collected by confocal scanning using the Roche NimbleGen MS200 Microarray Scanner at 2 μm pixel resolution (Roche NimbleGen). NimbleGen probe intensities were subjected to background correction, quantile normalization, and robust multiarray analysis as implemented in the NimbleScan Software, version 2.6 (Roche NimbleGen). Averaged gene-level signal intensities were summarized into gene calls and log2 transformed. The microarray data from this study have been deposited at the NCBI Gene Expression Omnibus (http://www.ncbi.nlm.nih.gov/geo/) under the accession number GSE52044.

RESULTS

Thrombin-Induced Redistribution of Tight and Adherens Junction Proteins

Tight and adherens junctions are key to maintaining and regulating the tightness of the endothelium. We investigated whether HUVECs were able to successfully establish tight and adherens junctions *in vitro* and whether those are affected by thrombin, a well-known vasoactive substance. Figure 1 shows the

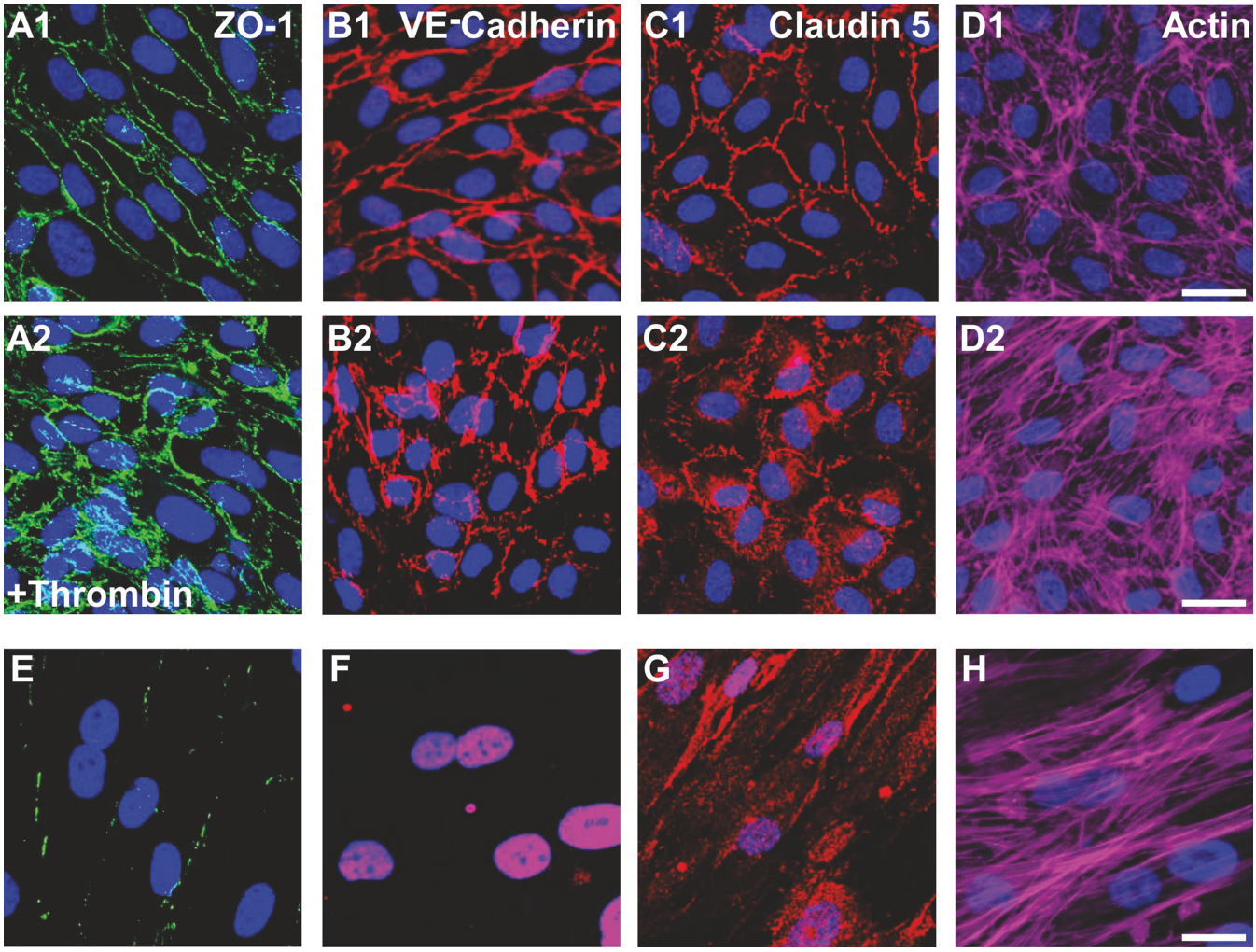

FIG. 1. Expression of junctional proteins: Immunocytochemistry of ZO-1, VE-Cadherin, and Claudin 5 on HUVECs with or without treatment of 20 U thrombin for 30 min (A1)–(D2) or CCD25-SK human fibroblasts (E)–(H). ZO-1, VE-Cadherin, and Claudin 5 staining clearly outline cell membranes of untreated HUVECs and actin staining is mostly restricted to the periphery of cell bodies (A1)–(D1). Thirty minutes after thrombin incubation, the ZO-1, VE-Cadherin, and Claudin 5 staining pattern is fragmented and actin stain shows a lot of filaments now located additionally at the center of the cell body (A2)–(D2). CCD25-SK human fibroblasts do not show any expression of ZO-1, VE-Cadherin, or Claudin 5 at cell membranes, and cells show a positive immunoreactivity for actin (E)–(H). Controls where primary antibody has been omitted do not show any unspecific binding. Scale bar = 25 μm.

expression pattern of three junctional proteins: VE-Cadherin, an adherens junction protein; Claudin 5, a tight junction protein; and ZO-1, a linker protein that links the tight junction proteins to the actin cytoskeleton (Vandenbroucke *et al.*, 2008). Under untreated conditions (Figs. 1A1–D1), tight and adherens junctional proteins were perfectly aligned along the cell membrane between neighboring HUVECs. Actin staining was concentrated at the periphery of each cell whereas the center around the nucleus did not show a pronounced actin staining. Thrombin was used as a positive control which is known to induce changes in vascular permeability (Baumer *et al.*, 2008; Rabiet *et al.*, 1996). Thirty minutes after thrombin was added, the expression pattern of the junctional proteins and actin changed significantly (see Figs. 1A2–D2). Staining of junctional proteins was not any longer aligned along membranes but was fragmented and even punctiform, signaling a disruption in the lining integrity and suggesting leakiness of the monolayer. Actin staining revealed an increase in actin positive fibers now as well present in the center of the cell. As expected, staining for ZO-1, VE-Cadherin, and Claudin 5 was negative along the membrane of CCD25-SK cells (Figs. 1E–G) confirming the absence of functional tight and adherens junction proteins in these fibroblasts.

Increase in Vascular Permeability Is Reflected by Decrease in Impedance

The next step was to investigate if impedance-based readout could monitor alterations of the vascular permeability induced

by thrombin. In contrast to the transwell assay, where an increase in permeability would lead to an increase in diffusion of a dye, an increase in vascular permeability would lead to a decrease in impedance in the presented system. We analyzed diffusion of FITC-labeled Dextran in a transwell assay with and without thrombin treatment and compared the results to those of the impedance assay. Diffusion of FITC-labeled Dextran through a confluent HUVEC monolayer did increase directly after treatment with thrombin whereas diffusion in untreated HUVECs was stable over all (see Fig. 2A). Dextran diffusion peaked at 45 min after thrombin treatment, decreased afterward continuously, and after 210 min the diffusion rate of thrombin-treated HUVECs was in the range of untreated controls. This finding was very well reproduced using impedance-based measurements. Time kinetic of the impedance curve mainly overlapped with that of the transwell assay where impedance showed a peak at around 45 min compared with an untreated cell and was reverted to the control level at around 210 min (Fig. 2B). We further investigated batch-to-batch variability of HUVECs with respect to their response to thrombin and IL-1β, a cytokine involved in induction of vascular leakage (Puhlmann *et al.*, 2005; Vandenbroucke *et al.*, 2008). Figures 2C and 2D show two different batches of HUVECs treated with 2 U/ml thrombin or 10 ng/ml IL-1β, respectively. Measured impedance of corresponding wells within one experiment was very consistent and showed low standard deviations between triplicates. Comparing impedance curves of two different HUVEC batches showed that the qualitative analysis of the impedance curve signature among batches was comparable despite small shifts in time course or curve maxima. However, this did not impact the assessment of an increase of vascular permeability compared with untreated controls.

Cytokine Receptor Expression in HUVECs

To further characterize and predict HUVEC responses to cytokines and thrombin, we investigated the expression profiles of corresponding receptors. As shown in Figure 3, HUVECs exhibited high mRNA expression levels of the thrombin receptor (F2R), the interferon gamma receptors 1 and 2 (IFNGR1, IFNGR2), and the TNF-α receptors 1A and 1B (TNFRSF1A, TNFRSF1B). The typeI interleukin 1 receptor (IL-1R1), which binds IL-1α and IL-1β, was moderately expressed together with its accessory transmembrane protein IL-1RAP. Not expressed were the type 2 interleukin 1 scavenger receptor (IL-1R2) and the heterotrimeric IL-2 receptor due to lack of expression of its alpha subunit (IL-2RA), and barely expressed beta (IL-2RB) and gamma (IL-2RG) subunits. The cytokine receptor complexes for IL-6 and IL-10 showed an imbalanced subunit expression. The IL-6 receptor (IL-6R) was moderately expressed whereas its subunit, the IL-6 signal transducer gp130 (IL-6ST), was 16-fold higher expressed. The IL-10 receptor alpha subunit showed low expression whereas the beta subunit was 12-fold higher expressed. Based on this expression profile, we expected substantial responses to TNF-α, IFN-γ, IL-1β, IL-6, IL-10, and thrombin, whereas we did not expect responses to IL-2.

Impedance-Based Analysis of Cytokine-Induced Changes in Vascular Permeability

We further investigated whether HUVECs were an adequate model to measure changes of vascular permeability by impedance technology. For this purpose, we treated a confluent monolayer of HUVECs growing on E-Plates 96 with cytokines or soluble factors for which we could demonstrate the presence of its corresponding receptor (see Fig. 3) and/or which were known to induce changes in vascular permeability. Impedance was measured continuously over the following 13 h. To ensure the specificity of our readout and to exclude compound-induced changes in impedance not due to a dysregulation of tight and/or adherens junction proteins, we compared side-by-side with a confluent monolayer of a human fibroblast cell line CCD25-SK. As shown before (see Fig. 1) CCD25-SK cells lack the expression of important adherens or tight junction proteins. Finally, to distinguish CI changes subsequent to decrease in cell viability, HUVECs were also treated with a cytotoxic agent (Triton X) and impedance curves were compared. Results were displayed as relative impedance changes to the untreated control.

First we analyzed thrombin, a compound which is known to alter the tightness of the endothelium by calcium-dependent mechanisms (Baumer *et al.*, 2008). HUVECs responded to low (0.2 U/ml) and intermediated (2 U/ml) doses of thrombin treatment by a fast, dose-dependent decrease of impedance, which was followed by a fast return to levels comparable to untreated cells. By contrast, using the highest dose (20 U/ml) of thrombin the impedance failed to fully recover and levels remained below that of untreated controls (see Fig. 4A). Importantly, human fibroblasts did not show a response to any of the three thrombin concentrations (Fig. 4A). Next, IL-1β, a cytokine that is able to induce vascular leakage (Capaldo and Nusrat, 2009), was assessed. At all three concentrations (1, 10, and 100 ng/ml) HUVECs treated with IL-1β showed a similar response of the impedance curve. Specifically, a sigmoid curve shape at the beginning followed by a continuous drop of CI was observed (see Fig. 4B). In contrast to HUVECs, IL-1β treatment of human fibroblasts did not lead to a significant decrease of impedance values (see Fig. 4B). Next, treatment of HUVECs with IFN-γ, another cytokine capable of inducing vascular leakage (Capaldo and Nusrat, 2009), led to a continuous decrease in impedance up to 5 h after treatment at 100, 1000, and 5000 U/ml followed by recovery to control levels within the following 5 h (Fig. 4C). CCD25-SK cells did not respond to IFN-γ incubation. TNF-α is also involved in increasing vascular permeability (Capaldo and Nusrat, 2009; Seybold *et al.*, 2005). HUVECs treated with TNF-α respond with a similar impedance curve pattern at 10, 100, and 500 ng/ml like those treated with IL-1β (Fig. 4D). In contrast to that CCD25-SK cells responded to TNF-α treatment with a slight drop in impedance which went up to control levels after 10 h (Fig. 4D). In summary, impedance analysis of TNF-

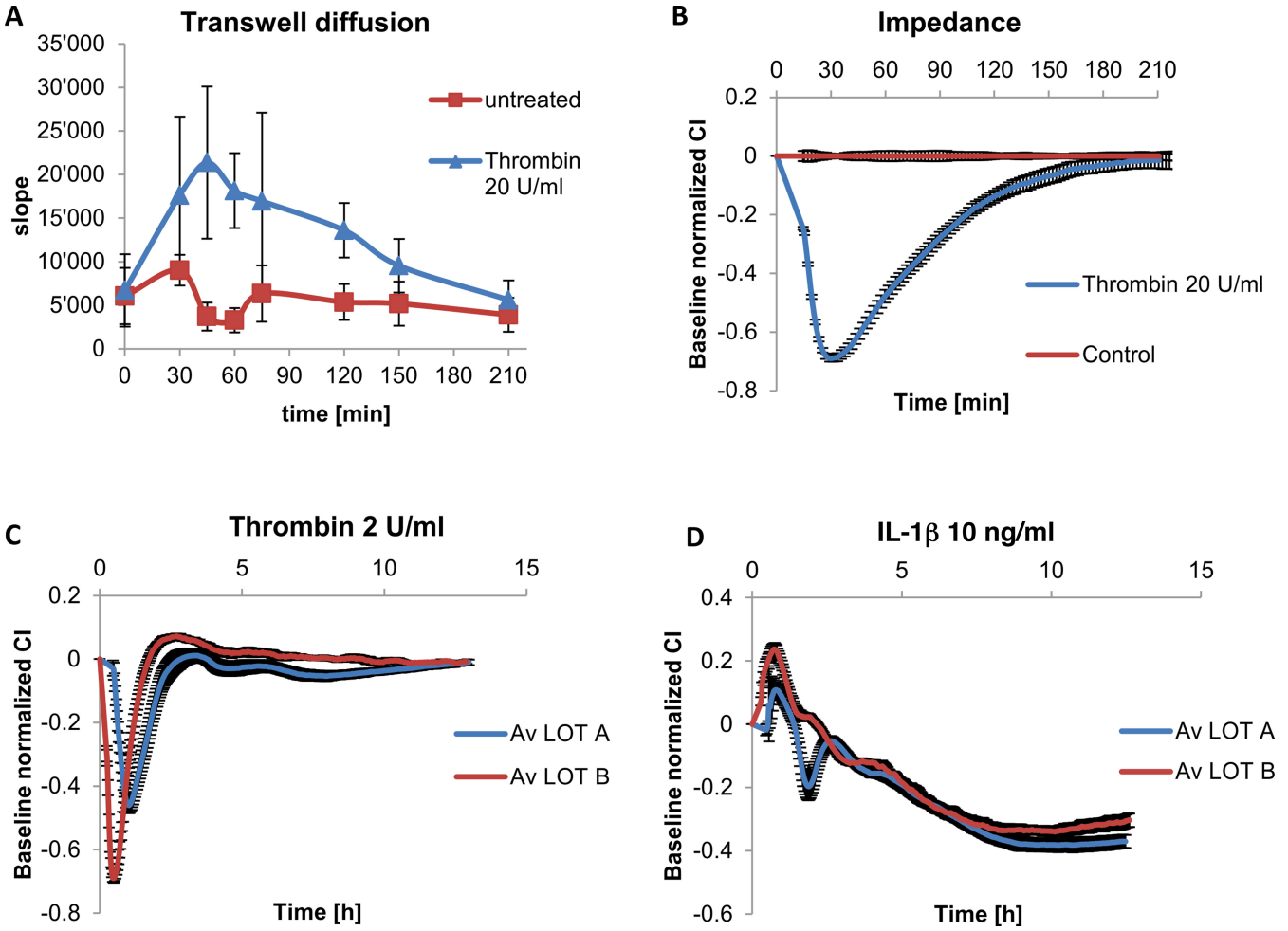

FIG. 2. Comparison of a transwell diffusion assay and an impedance assay (A) and (B), and batch-to-batch variability of the impedance assay (C) and (D). Time kinetics of diffusion of FITC-labelled Dextran through a monolayer of confluent HUVECs (A) is comparable to that of the impedance-based analysis (B), i.e., an increasing loss of barrier integrity within the first 60 min followed by a decrease back to control levels after 3 h. Comparison of batch-to-batch variability using two different batches of HUVECs treated with either thrombin (C) or IL-1β (D) at similar conditions shows that the quality of the readout is comparable between different batches and both show a decrease in impedance with comparable time kinetics after treatment. Displayed are the average of $n = 3$ biological replicates for (A), $n = 4$ for (B), $n = 6$ (LOT A) for (C) and (D), and $n = 4$ (LOT B) for (C) and (D), and each value is displayed ± standard deviation.

α, IFN-γ, IL-1β, and thrombin was well in line with receptor expression data (see Fig. 3) which suggested a positive response of HUVECs due to treatment with these cytokines and soluble factors.

Second IL-2 and IL-6 were analyzed, both cytokines that play a role in increasing vascular permeability as well (Capaldo and Nusrat, 2009). Impedance analysis of IL-2 at 10, 100, and 500 ng/ml was well in line with the receptor expression profiles of HUVECs (see Fig. 3) which suggested no response to IL-2 treatment due to a lack of the corresponding receptors. Indeed, both in HUVECs and in CCD25-SK cells we could not measure any change in impedance after IL-2 treatment (see Fig. 4E). Unexpectedly, for IL-6 at 10, 100, and 500 ng/ml we could not measure any response of the impedance readout after IL-6 treatment (see Fig. 4F), which was in contrast to the positive expression of IL-6 receptors (see Fig. 3).

IL-10 is normally involved in increasing the tightness of the vasculature (Capaldo and Nusrat, 2009; Oshima *et al.*, 2001). According to this, incubation of HUVECs with IL-10 at 10, 100, and 500 ng/ml did not lead to a decrease of impedance but impedance remained stable apart from a short drop which was fully reversible at the very beginning of the analysis (Fig. 4G). Fibroblasts incubated with IL-10 also did not respond to treatment and impedance levels stayed constant over time (Fig. 4G). Finally, treatment of fibroblasts and HUVECs with a detergent Triton X 100 at 0.01, 0.1, and 1% did lead to a drop of impedance in both cell models in the same way, indicative of a cell-type unspecific cytotoxic effect. Whereas the low concentration of Triton X 100 did induce only a slight drop of

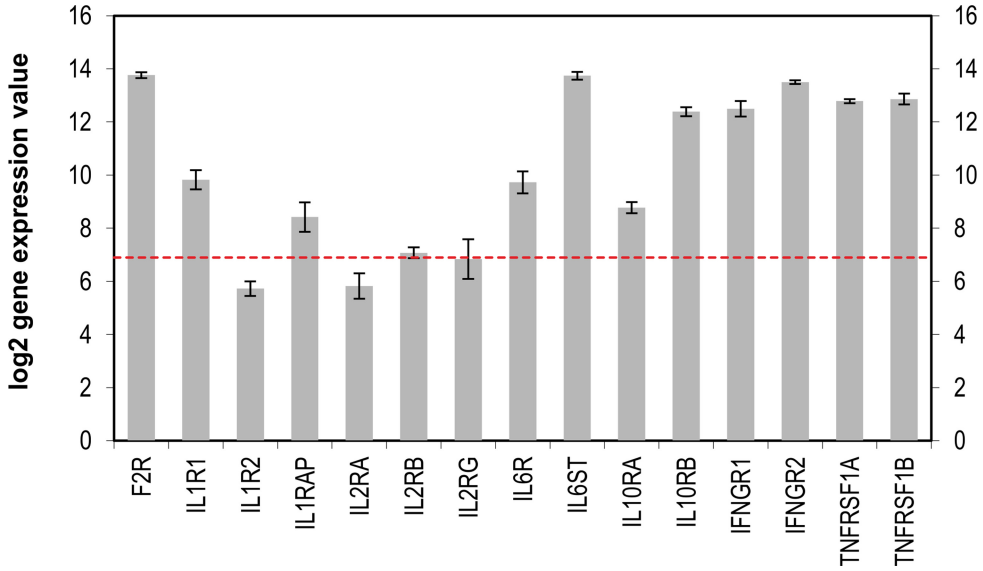

FIG. 3. Receptor expression in HUVECs. Gene expression signals of thrombin and cytokine receptors showing mean and standard deviations of three different HUVEC batches. The detection limit of the microarray platform is indicated by a red dotted line; this signal is derived from 5000 random probes (60 mers of random nucleotides), which serve as a metric of nonspecific annealing and background fluorescence.

impedance, the middle and the high dose led to an immediate, irreversible drop of impedance (Fig. 4H).

Induced Vascular Permeability Could Be Reverted by Specific Antagonists

The final step of assessing the impedance analysis was whether nonspecific and specific antagonists of vascular leak could prevent or revert drops in impedance following classical inducers. First, histamine induced a short, strong, and fully reversible drop of the impedance (see Fig. 5A, blue line). Pretreatment of HUVECs with methylprednisolone 12 h before histamine was added (time point histamine was added is indicated with "1" in Fig. 5A) fully inhibited the histamine-induced drop of the impedance curve (see Fig. 5A, red line). However, adding methylprednisolone (time point methylprednisolone was added is indicated with "3" in Fig. 5A) to HUVECs which had already been cultured with histamine (time point histamine was added is indicated with "2" in Fig. 5A) did not revert the impedance effect of histamine (compare the blue line and the green line in Fig. 5A). Administration of clemastine, a histamine receptor 1 antagonist (Peck *et al.*, 1975), 12 h before histamine stimulation of HUVECs (time point clemastine was added is indicated with "1" in Fig. 5B) fully abolished the drop of impedance by histamine (time point histamine was added is indicated with "2" in Fig. 5B, red line). Like with methylprednisolone, addition of clemastine to HUVECs (time point clemastine was added is indicated with "3" in Fig. 5B) which had already been incubated with histamine did not alter the impedance curve (Fig. 5B, green line). Likewise, the IL-1β-induced drop of impedance could be abrogated by a pretreatment of HUVECs with anakinra, an IL-1 receptor antagonist (Fig. 5C, red line; Cohen *et al.*, 2003). Furthermore, addition of anakinra to HUVECs which had been treated with IL-1β before, led to reversion of the IL-1-induced effect (Fig. 5C, green line). The TNF-α-induced drop of impedance could be completely abrogated by pretreatment of HUVECs with Remicade, a neutralizing monoclonal antibody against human TNF-α (Fig. 5D, red line; Maini *et al.*, 1998). Addition of Remicade to HUVECs which had already been incubated with TNF-α led to a rescue and impedance went up to control level (Fig. 5D, green line). High content analysis at the end of the experiment for cell death did not show a significant increase in cell death due to the different compounds analyzed by a one-way ANOVA (analysis of variance) and a Dunnett post-test.Apart from TNF-α alone, none of the other treatments increased the percentage of dead cell content per well compared with the untreated controls (Fig. 5E). However, the fact that the impedance curve after addition of Remicade reached a level comparable to that of pretreated conditions strongly suggests real functional antagonism rather than differences in the dead cell content.

DISCUSSION

The goal of the present study was to design an *in vitro* system to accurately assess the ability of a therapeutic compound to alter the endothelial monolayer integrity. In order to predict vascular leak *in vivo* we established a reliable and rapid *in vitro* assay using HUVECs as a model of the endothelium. We could demonstrate their relevance because they expressed major junctional proteins responsible for maintaining the tightness of the endothelium including receptors for most cytokines re-

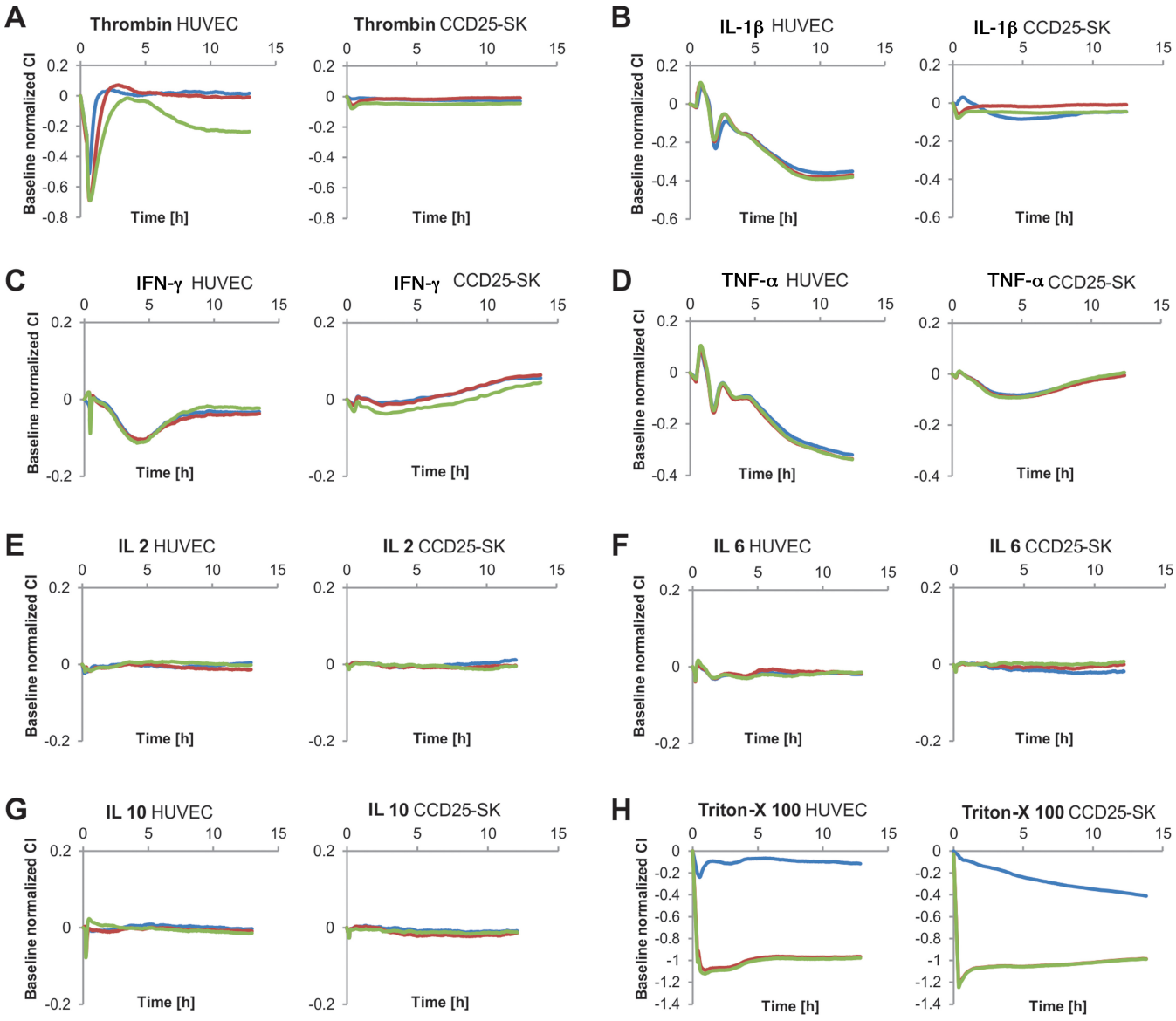

FIG. 4. Impedance-based vascular leakage assay: Impedance based analysis for vascular leakage induced by thrombin, IL-1β, IFN-γ, TNF-α, IL-2, IL-6, IL-10, and Triton-X 100. HUVECs or CCD25-SK as a nonresponder cell line are incubated with the different compounds at three different concentration (for details please refer to the Materials and Methods section): low concentration (blue line), medium concentration (red line), and high concentration (green line), and impedance was continuously measured the following hours. Each line represents the average of one experiment with $n = 6$ biological replicate wells (except for (H) HUVEC $n = 4$). Each experiment has been repeated twice and graphs are representative for both experiments.

sponsible for increased vascular permeability. We introduced an impedance-based platform to capture compound induced changes in endothelial barrier function and could prove that results were fully concordant to those measured by a standard transwell chamber vascular permeability assay. In addition, our assay is a noninvasive, highly reproducible method that allows real-time kinetics, dose-effect comparison, parallel recording of different treatments, and semiquantitative assessment relative to controls in a very efficient way. Our assay approach included testing compounds in parallel on nonresponder human fibroblast cells which did increase specificity to predict vascular leakage by excluding direct cytotoxic events underlying the impedance curve changes. Furthermore, by treatment of cells with antagonists for histamine, IL-1β, or TNF-α we could completely block the impedance drop *in vitro* and IL-1β or TNF-α-induced vascular leakage could even be reverted by addition of rheumatoid arthritis drugs anakinra or Remicade to the cells. This further underlines the biological relevance of the established assay in terms of the chosen cellular model HUVEC as

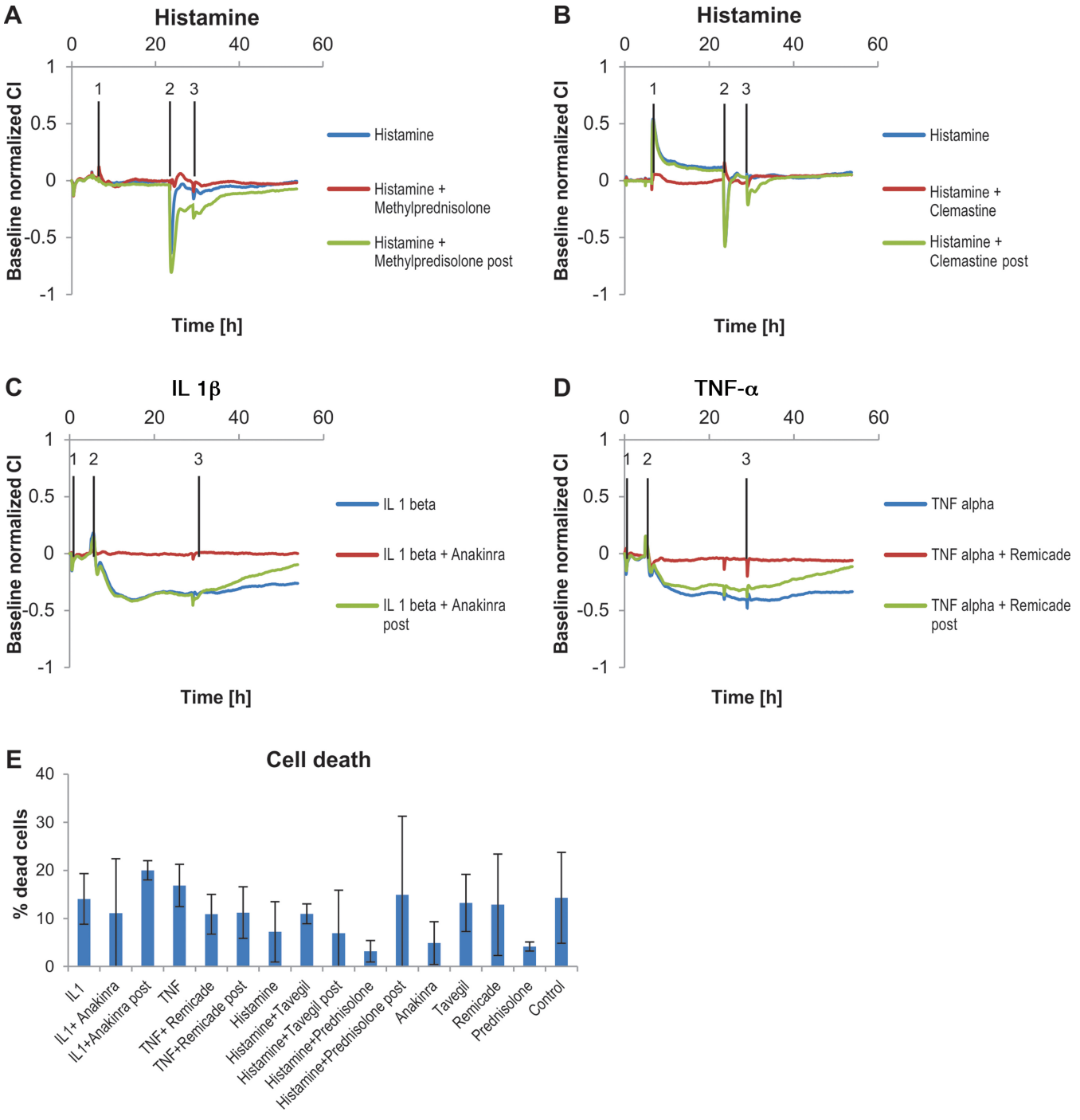

FIG. 5. Antagonization of vascular leakage by antagonists: Antagonization of histamine, IL-1β, or TNF-α-induced vascular permeability. HUVECs are treated with histamine, IL-1β, or TNF-α [indicated as "2" in (A)–(D)], which induces vascular leakage [blue line; (A)–(D)]. Vascular leakage shown as decrease impedance values is abrogated by a preceding addition of the corresponding antagonist at time point "1" [red line; (A)–(D)]. Post-treatment of HUVECs after incubation with histamine, IL-1β, or TNF-α with the corresponding antagonists at time point "3" does not revert the histamine effect but that of IL-1β and TNF-α, where impedance levels increase back to pretreatment levels [green line; (A)–(D)]. Displayed is the average of $n = 4$ biological replicates for each experiment. (E) Cytotoxicity analysis using high-content imaging 24 h after post-treatment of cells with the corresponding antagonist as shown in (A)–(D) reveals that only incubation of HUVECs with TNF-α alone increases the number of dead cells compared with controls. Any other treatment is not raising the number of dead cells compared with untreated controls. Displayed are the average values of $n = 4$ biological replicates ± standard deviation.

well as the real-time, impedance-based readout to predict clinically relevant drug-induced vascular permeability.

In mammals, proinflammatory cytokines and other vasoactive substances have been shown to increase permeability of the endothelium by directly interacting with receptors on the surface of endothelial cells (Capaldo and Nusrat, 2009). Through various mechanisms this may lead to a disassembly of cell-cell junctional proteins and to remodeling of the actin cytoskeleton which are considered key events in the early stages of vascular leakage (Vandenbroucke *et al.*, 2008). In our model, we could demonstrate that HUVECs successfully establish tight and adherens junctions revealed by an expression of ZO-1, VE-Cadherin, and Claudin 5 which is in concordance with previously published work using HUVECs as a model of the endothelium (Baumer *et al.*, 2010) underlying the relevance of our established *in vitro* system. After incubation with thrombin for 30 min HUVECs displayed fragmentation of tight and adherens junction expression pattern as revealed by a ZO-1, VE-Cadherin, and Claudin 5 staining (Fig. 1). Additionally, actin staining revealed appearance of multiple stress fibers (Fig. 1D) which is in line with previous data as well demonstrating fragmentation of VE-Cadherin staining and increase in actin stress fibers in human dermal microvascular endothelial cells upon thrombin treatment (Baumer *et al.*, 2008).

Multiple cytokines and other soluble factors have been identified which could induce vascular permeability, including IL-2 and IL-6 (Capaldo and Nusrat, 2009). Although the *in vivo* effect of IL-1β, TNF-α, IFN-γ, histamine, and thrombin could be recapitulated in our model, an increase of vascular permeability using IL-2 or IL-6 could not be observed (Fig. 4). With respect to IL-2, this result is in line with previously published and with our current data showing lack of IL-2 receptor expression on HUVECs (Dewi *et al.*, 2004). Additionally, it is still not fully established whether IL-2-induced vascular leakage is due to direct interaction with endothelial cells or indirectly via interaction of IL-2 via activated neutrophils, which were not present in our assay system (Baluna, 2007; Capaldo and Nusrat, 2009). The lack of response of HUVECs to IL-6 is in contrast to another publication demonstrating IL-6-mediated increase in permeability (Desai *et al.*, 2002) and also not in line with our data showing IL-6 receptor subunit expression on the cells. It could be speculated that HUVECs used in the present system do not allow efficient IL-6 receptor complex assembly due to imbalanced expression of the receptor subunits or due to a lack in lipid rafts or protein sorting into lipid rafts, which is necessary for proper IL-6 signaling (Buk *et al.*, 2005).

In contrast to other approaches aiming to assess vascular permeability relying on endothelial cells only (Ludwig *et al.*, 2011), we have included here a negative control cell model, i.e., human skin fibroblasts, which do not express Claudin 5 or VE-Cadherin (Fig. 1; Furuse *et al.*, 1998). Thus, comparison of impedance curves of HUVECs versus fibroblasts was used to exclude unspecific effects on cellular morphology by processes other than those affecting cell-cell junctions. Incubation of fibroblasts with cytokines or thrombin did not alter impedance confirming that modulation of cell-cell junctions in HUVECs reflects a key step in the development of vascular leakage. It should be noted though that IFN-γ did induce a slight increase in impedance which is normally indicative of increase proliferation compared with control. This observation is in line with a publication describing an increase in proliferation of slowly dividing fibroblasts after IFN-γ treatment (Elias *et al.*, 1987). We propose that it is an effect on fibroblast morphology rather than a true proliferative response, which is supported by the fact that fibroblast cultures were confluent at the time point of treatment making an increase of proliferation unlikely. Thus, our results demonstrate the importance of including an additional cell model which serves as a negative control to exclude unspecific effects.

A key aspect of the present study was to show physiological relevance and specificity of the model by being able to inhibit or reverse vascular leakage induced by histamine, IL-1β, or TNF-α using established drugs (Fig. 5). Only for histamine we could not revert the effect by addition of either methylprednisolone or clemastine directly after histamine treatment to the cells. On the other hand, pretreatment of HUVECs with Methylpredisolone and clemastine did completely inhibit leakage. The lack of response might be due to a very short half-life of the histamine effect per se where the induced leakage is back to control levels already 90 min after the onset of the effect. Given this, it would be almost impossible to revert such an effect on an *in vitro* level. Additional analysis of cytotoxicity revealed that both inducers and inhibitors of vascular leakage did not induce a significant effect as shown by HCI (high content imaging) analysis further excluding unspecific changes introducing bias.

Taken together, the present study shows for the first time a comprehensive analysis of several cytokines and an additional soluble factor for the induction of vascular permeability using impedance analysis. HUVECs in combination with impedance measurements are a well-suited model to measure increase in vascular leakage in real time. By including fibroblasts devoid of junction proteins, we were able to differentiate endothelial-cell specific from unspecific cellular effects. Additionally, we were able to specifically revert the induction of vascular leakage using established antagonists. The assay is simple to use and showed excellent reproducibility with a meaningful throughput. In biopharmaceutical industry, it could be used to test drug candidates for their potential to induce vascular leakage via direct effects on endothelial cells. Additionally, our approach has shown its applicability to test clinically relevant counter measures for a drug-induced vascular leakage. The platform also bears the potential to be adapted to several target organs: e.g., it could be used to test drug-induced vascular leakage in the eye which bears a high risk for induction of severe visual impairment by inducing macular edema (Makri *et al.*, 2013). Thus, impedance-based analysis of vascular leakage is a well suited tool to test drugs for their potential to increase vascular leakage early on in drug development.

ACKNOWLEDGMENTS

We would like to thank Eduard Urich for his support with the setup of the transwell assay, Karen Dernick and Christine Zihlmann for cell culture work and HCI analysis. *Conflict of interest statement.* The authors are or were employees of F. Hoffmann-La Roche Ltd. They declare no conflicts of interest.

REFERENCES

Aghajanian, A., Wittchen, E. S., Allingham, M. J., Garrett, T. A., and Burridge, K. (2008). Endothelial cell junctions and the regulation of vascular permeability and leukocyte transmigration. *J. Thromb. Haemost.* **6**, 1453–1460.

Baluna, R. G. (2007). Cytokine-induced vascular leak syndrome. In *Cytokines in Human Health: Immunotoxicology, Pathology, and Therapeutic Applications (Methods in Pharmacology and Toxicology)* (R. V. House and J. Descotes, Eds.), pp. 205–231, Humana Press Inc., Totowa, NJ.

Baumer, Y., Burger, S., Curry, F. E., Golenhofen, N., Drenckhahn, D., and Waschke, J. (2008). Differential role of Rho GTPases in endothelial barrier regulation dependent on endothelial cell origin. *Histochem. Cell Biol.* **129**, 179–191.

Baumer, Y., Funk, D., and Schlosshauer, B. (2010). Does telomerase reverse transcriptase induce functional de-differentiation of human endothelial cells? *Cell. Mol. Life Sci.* **67**, 2451–2465.

Bazzoni, G. (2006). Endothelial tight junctions: Permeable barriers of the vessel wall. *Thromb. Haemost.* **95**, 36–42.

Buk, D. M., Renner, O., and Graeve, L. (2005). Increased association with detergent-resistant membranes/lipid rafts of apically targeted mutants of the interleukin-6 receptor gp80. *Eur. J. Cell Biol.* **84**, 819–831.

Capaldo, C. T.,, and Nusrat, A. (2009). Cytokine regulation of tight junctions. *Biochim. Biophys. Acta* **1788**, 864–871.

Cohen, S. B., Woolley, J. M., and Chan, W. (2003). Interleukin 1 receptor antagonist anakinra improves functional status in patients with rheumatoid arthritis. *J. Rheumatol.* **30**, 225–231.

Desai, T. R., Leeper, N. J., Hynes, K. L., and Gewertz, B. L. (2002). Interleukin-6 causes endothelial barrier dysfunction via the protein kinase C pathway. *J. Surg. Res.* **104**, 118–123.

Dewi, B. E., Takasaki, T., and Kurane, I. (2004). In vitro assessment of human endothelial cell permeability: Effects of inflammatory cytokines and dengue virus infection. *J. Virol. Methods* **121**, 171–180.

Dudek, S. M.,, and Garcia, J. G. (2001). Cytoskeletal regulation of pulmonary vascular permeability. *J. Appl. Physiol.* **91**, 1487–1500.

Elias, J. A., Jimenez, S. A., and Freundlich, B. (1987). Recombinant gamma, alpha, and beta interferon regulation of human lung fibroblast proliferation. *Am. Rev. Respir. Dis.* **135**, 62–65.

Furuse, M., Sasaki, H., Fujimoto, K., and Tsukita, S. (1998). A single gene product, claudin-1 or -2, reconstitutes tight junction strands and recruits occludin in fibroblasts. *J. Cell Biol.* **143**, 391–401.

Kovacs, J. A., Baseler, M., Dewar, R. J., Vogel, S., Davey, R.T., Jr, Falloon, J., Polis, M. A., Walker, R. E., Stevens, R., and Salzman, N. P. (1995). Increases in CD4 T lymphocytes with intermittent courses of interleukin-2 in patients with human immunodeficiency virus infection. A preliminary study. *N. Engl. J. Med.* **332**, 567–575.

Lotze, M. T., Matory, Y. L., Rayner, A. A., Ettinghausen, S. E., Vetto, J. T., Seipp, C. A., and Rosenberg, S. A. (1986). Clinical effects and toxicity of interleukin-2 in patients with cancer. *Cancer* **58**, 2764–2772.

Ludwig, A., Sommer, A., and Uhlig, S. (2011). Assessment of endothelial permeability and leukocyte transmigration in human endothelial cell monolayers. *Methods Mol. Biol.* **763**, 319–332.

Maini, R. N., Breedveld, F. C., Kalden, J. R., Smolen, J. S., Davis, D., Macfarlane, J. D., Antoni, C., Leeb, B., Elliott, M. J., and Woody, J. N. (1998). Therapeutic efficacy of multiple intravenous infusions of anti-tumor necrosis factor alpha monoclonal antibody combined with low-dose weekly methotrexate in rheumatoid arthritis. *Arthritis Rheum.* **41**, 1552–1563.

Makri, O. E., Georgalas, I., and Georgakopoulos, C. D. (2013). Drug-induced macular edema. *Drugs* **73**, 789–802.

Oshima, T., Laroux, F. S., Coe, L. L., Morise, Z., Kawachi, S., Bauer, P., Grisham, M. B., Specian, R. D., Carter, P., and Jennings, S. (2001). Interferon-gamma and interleukin-10 reciprocally regulate endothelial junction integrity and barrier function. *Microvasc. Res.* **61**, 130–143.

Peck, A. W., Fowle, A. S., and Bye, C. (1975). A comparison of triprolidine and clemastine on histamine antagonism and performance tests in man: Implications for the mechanism of drug induced drowsiness. *Eur. J. Clin. Pharmacol.* **8**, 455–463.

Puhlmann, M., Weinreich, D. M., Farma, J. M., Carroll, N. M., Turner, E. M., and Alexander, H. R., Jr, (2005). Interleukin-1beta induced vascular permeability is dependent on induction of endothelial tissue factor (TF) activity. *J. Transl. Med.* **3**, 37. doi: 10.1186/1479–5876–3–37.

Rabiet, M. J., Plantier, J. L., Rival, Y., Genoux, Y., Lampugnani, M. G., and Dejana, E. (1996). Thrombin-induced increase in endothelial permeability is associated with changes in cell-to-cell junction organization. *Arterioscler. Thromb. Vasc. Biol.* **16**, 488–496.

Seybold, J., Thomas, D., Witzenrath, M., Boral, S., Hocke, A. C., Burger, A., Hatzelmann, A., Tenor, H., Schudt, C., and Krull, M. (2005). Tumor necrosis factor-alpha-dependent expression of phosphodiesterase 2: Role in endothelial hyperpermeability. *Blood* **105**, 3569–3576.

Siegel, J. P.,, and Puri, R. K. (1991). Interleukin-2 toxicity. *J. Clin. Oncol.* **9**, 694–704.

Suntharalingam, G., Perry, M. R., Ward, S., Brett, S. J., Castello-Cortes, A., Brunner, M. D., and Panoskaltsis, N. (2006). Cytokine storm in a phase 1 trial of the anti-CD28 monoclonal antibody TGN1412. *N. Engl. J. Med.* **355**, 1018–1028.

Vandenbroucke, E., Mehta, D., Minshall, R., and Malik, A. B. (2008). Regulation of endothelial junctional permeability. *Ann. N. Y. Acad. Sci.* **1123**, 134–145.